SEISMIC PERFORMANCE OF BRIDGE COLUMNS WITH INTERLOCKING SPIRAL REINFORCEMENT

WA-RD 357.1

Final Report
September 1994

Washington State Department of Transportation

Washington State Transportation Commission
Planning and Programming Service Center
in cooperation with the U.S. Department of Transportation
Federal Highway Administration

TECHNICAL REPORT STANDARD TITLE PAGE

1. REPORT NO.	2. GOVERNMENT ACCESSION NO.	3. RECIPIENT'S CATALOG NO.
WA-RD 357.1		

4. TITLE AND SUBTITLE	5. REPORT DATE
Seismic Performance of Bridge Columns with Interlocking Spiral Reinforcement	September 1994
	6. PERFORMING ORGANIZATION CODE
7. AUTHOR(S)	8. PERFORMING ORGANIZATION REPORT NO.
David I. McLean and Grant C. Buckingham	
9. PERFORMING ORGANIZATION NAME AND ADDRESS	10. WORK UNIT NO.
Washington State Transportation Center (TRAC) Civil and Environmental Engineering; Sloan Hall, Room 101 Washington State University Pullman, Washington 99164	11. CONTRACT OR GRANT NO. GC8720-14
12. SPONSORING AGENCY NAME AND ADDRESS	13. TYPE OF REPORT AND PERIOD COVERED
Washington State Department of Transportation Transportation Building, MS 7370 Olympia, Washington 98504-7370	Final Technical Report
	14. SPONSORING AGENCY CODE

15. SUPPLEMENTARY NOTES

This study was conducted in cooperation with the U.S. Department of Transportation, Federal Highway Administration.

16. ABSTRACT

Transverse reinforcement in bridge columns normally consists of spiral reinforcement in columns with circular cross-sections and tied reinforcement in columns with square or rectangular cross-sections. The circular shape of spiral reinforcement is inherently efficient in providing confinement to the concrete core and restraint of longitudinal bar buckling. In contrast, rectangular columns require cross-ties and/or overlapping ties in addition to the perimeter tie in order to provide adequate confinement and restraint of bar buckling. As an alternative reinforcing scheme, interlocking spiral reinforcement has been used in California for columns with rectangular cross-sections. However, several important design elements are not addressed in the Caltrans specifications, and the performance of columns with interlocking spirals has not been fully established.

This study experimentally investigated the seismic behavior of columns incorporating interlocking spirals under flexural, shear and torsional loadings. The main tests were performed on approximately 1/5-scale column specimens subjected to increasing levels of cycled inelastic displacements under constant axial load. Rectangular and oval cross-sections with either two interlocking spirals or conventional ties were investigated. Variables studied included the performance of interlocking spirals compared to ties, the amount of spiral overlap, and the size of longitudinal bars required in the overlap region to maintain spiral interlock.

Columns with interlocking spirals performed as well or better than columns with ties, despite approximately 50% more transverse reinforcement being provided in the tied columns. Test results indicated improved performance when the center-to-center spacing of interlocking spirals was not greater than 0.6 times the spiral diameter. At least four longitudinal bars of approximately the same size as the main longitudinal reinforcement are required in the overlap region to maintain spiral interlock. Procedures were developed for predicting the axial, shear, flexural and torsional strengths of columns with the interlocking spirals.

17. KEY WORDS	18. DISTRIBUTION STATEMENT
Seismic design, bridges, columns, reinforced concrete, transverse reinforcement.	No restrictions. This document is available to the public through the National Technical Information Service, Springfield, VA 22616

19. SECURITY CLASSIF. (of this report)	20. SECURITY CLASSIF. (of this page)	21. NO. OF PAGES	22. PRICE
None	None	50	

Final Report

Research Project GC 8720-14
Column Confinement Reinforcement

SEISMIC PERFORMANCE OF BRIDGE COLUMNS WITH INTERLOCKING SPIRAL REINFORCEMENT

by

David I. McLean
Associate Professor

Grant C. Buckingham
Graduate Student

Washington State Transportation Center (TRAC)
Department of Civil and Environmental Engineering
Washington State University
Pullman, Washington 99164-2910

Washington State Department of Transportation
Technical Monitor
C. Ernest Nelson
Bridge and Structures Branch Supervising Bridge Engineer

Prepared for

Washington State Transportation Commission
Department of Transportation
and in cooperation with
U.S. Department of Transportation
Federal Highway Administration

September 1994

DISCLAIMER

The contents of this report reflect the views of the authors, who are responsible for the facts and the accuracy of the data presented herein. The contents do not necessarily reflect the official views or policies of the Washington State Transportation Commission, Department of Transportation, or the Federal Highway Administration. This report does not constitute a standard, specification, or regulation.

TABLE OF CONTENTS

LIST OF FIGURES

LIST OF TABLES

SUMMARY

Transverse reinforcement in bridge columns normally consists of spiral reinforcement in columns with circular cross-sections and tied reinforcement in columns with square or rectangular cross-sections. The circular shape of spiral reinforcement is inherently efficient in providing confinement to the concrete core and restraint of longitudinal bar buckling. In contrast, rectangular columns require cross-ties and/or overlapping ties in addition to the perimeter tie in order to provide adequate confinement and restraint of bar buckling. Hence, tied columns are often more difficult to construct and require larger amounts of transverse reinforcement than columns with spiral reinforcement. As an alternative reinforcing scheme, interlocking spiral reinforcement has been used in California for columns with rectangular cross-sections. However, several important design elements are not addressed in the Caltrans specifications, and the performance of columns with interlocking spirals has not been fully established.

This study experimentally investigated the seismic behavior of columns incorporating interlocking spirals under flexural, shear and torsional loadings. The main tests were performed on approximately 1/5-scale column specimens subjected to increasing levels of cycled inelastic displacements under constant axial load. Rectangular and oval cross-sections with either two interlocking spirals or conventional ties were investigated. Variables studied included the performance of interlocking spirals compared to ties, the amount of spiral overlap, and the size of longitudinal bars required in the overlap region to maintain spiral interlock. Column

performance was evaluated in terms of lateral load capacity, strength degradation, energy dissipation, and failure mechanisms.

Columns with interlocking spirals performed as well or better than columns with ties, despite approximately 50% more transverse reinforcement being provided in the tied columns. Test results indicated improved performance when the center-to-center spacing of interlocking spirals was not greater than 0.6 times the spiral diameter. At least four longitudinal bars of approximately the same size as the main longitudinal reinforcement are required in the overlap region to maintain spiral interlock. When adequate longitudinal bars and spiral overlap were provided, the spirals remained interlocked even when loaded to large displacements thus preserving load transfer between the spirals. Procedures were developed for predicting the axial, shear, flexural and torsional strengths of columns with the interlocking spirals.

CONCLUSIONS AND RECOMMENDATIONS

CONCLUSIONS

On the basis of the results of this experimental investigation, the following conclusions are made:

1. Specimens constructed with interlocking spirals for transverse reinforcement performed as well or better than specimens with ties under both shear and flexural loading, despite the fact that the specimens reinforced with ties contained 50% more transverse reinforcement than the specimens with interlocking spirals.

2. When loaded to failure in shear, the specimen incorporating a spiral overlap of 25% (center-to-center spacing of spirals equal to 0.6 times the spiral diameter) demonstrated better energy dissipation characteristics and less strength degradation than the similar specimen incorporating a spiral overlap of 15% (center-to-center spacing of spirals equal to 0.75 times the spiral diameter). Failure in the specimen with the 15% overlap was caused by rupture of the spiral reinforcement, whereas failure in the specimen with the 25% overlap was a result of gradual deterioration of the concrete core of the column.

3. The use of small-diameter (nominal) longitudinal bars in the interlock region resulted in higher degradation and lower energy dissipation when compared to the similar specimen with the same size of longitudinal bars in the interlock region as that used for the main column reinforcement. The reduced performance of the specimen using nominal interlock bars was due to separation of the spiral cages resulting from severe deformation of the interlock bars.

4. The axial, shear and flexural capacities of columns with interlocking spirals can be accurately predicted using current procedures for the design of reinforced concrete structures. The torsional capacity of columns with interlocking spirals can be conservatively predicted using an approach adapted from current design equations for the torsional capacity of rectangular beams.

RECOMMENDATIONS

The following recommendations are made based on the results of this study and a survey of literature.

1. The center-to-center spacing of adjacent spirals in columns with interlocking spirals should not exceed 0.6 times the diameter of the spiral cage.

2. At least four longitudinal bars of approximately the same size as the main longitudinal reinforcement should be incorporated into the interlock region to prevent separation of the individual spiral cages.

3. Current equations for determining the required volume of spiral reinforcement in circular columns can be applied to columns with interlocking spirals provided that each spiral in the column is treated individually.

4. Further research is recommended on the torsional behavior of columns with interlocking spirals, particularly in regard to rotation-direction bias resulting in unwinding of the spirals. It is also recommended that the behavior of columns with more than two interlocking spirals be investigated.

INTRODUCTION

INTRODUCTION AND BACKGROUND

Transverse reinforcement in bridge columns normally consists of spiral reinforcement in columns with circular cross-sections and tied reinforcement in columns with square or rectangular cross-sections. The circular shape of spiral reinforcement is inherently efficient in providing confinement to the concrete core and restraint of longitudinal bar buckling. In contrast, rectangular columns require cross-ties and/or overlapping ties in addition to the perimeter tie in order to provide adequate confinement and restraint of bar buckling. As a result, tied columns are often more difficult to construct and require larger amounts of transverse reinforcement than columns with spiral reinforcement.

In order to incorporate the benefits of spiral reinforcement into non-circular columns, the California Department of Transportation (Caltrans) has implemented the use of interlocking spirals. The volume of transverse reinforcement in columns with interlocking spirals is normally less than that for columns with ties. The seismic performance of columns with interlocking spirals may also be superior to that for tied columns. However, the performance of columns with interlocking spirals has not been fully established.

The Caltrans specifications (1) contains provisions for the design of columns with interlocking spirals. However, most of the design provisions are apparently based on specifications for single spiral columns with circular cross-sections, which may not be adequate for interlocking spiral columns. Further, several important

design elements are not addressed in the specifications. Additional information on the behavior of columns with interlocking spirals must be obtained in order to determine specific design requirements.

RESEARCH OBJECTIVES

The objectives of this study were as follows:

1. to experimentally investigate the behavior of columns incorporating interlocking spiral reinforcement under shear, flexural and torsional loading;
2. to study the effects of several design variables on the behavior of columns with interlocking spirals, including transverse reinforcement requirements, size of longitudinal bars in the interlock zone, and flexural detailing of interlocking spirals in rectangular columns;
3. to compare the performance of columns with interlocking spirals to columns with ties;
4. to develop methods for predicting the shear, flexural, torsional and axial capacities of columns with interlocking spirals; and
5. to make recommendations for the design of bridge columns incorporating interlocking spirals as the transverse reinforcement.

LITERATURE REVIEW

DESIGN CRITERIA FOR COLUMNS WITH INTERLOCKING SPIRALS

Amount of Spiral Overlap

In order for a column with interlocking spirals to resist shear forces, an efficient transfer of these forces from spiral-to-spiral must take place. Tanaka and Park (2) developed a subjective approach to ensure force transfer by requiring that the amount of spiral overlap be such that the component of spiral force parallel to the direction of loading at the point of spiral intersection is no less than 80% of the yield force of the spiral. This standard results in a maximum allowable spacing between centers of adjacent spirals of $1.2r_1$, where r_1 is the radius of the spiral reinforcement. This criteria also corresponds to a minimum spiral overlap of 25%, where the overlap percentage is defined as the depth of the interlock region divided by the total depth of the transverse reinforcement.

The Caltrans specifications (1) sets the maximum allowable value for center-to-center spacing of adjacent spirals at "0.75 times the diameter of the cage," or $1.5r_1$. The Caltrans criteria corresponds to a minimum spiral overlap of 14.3%.

Maintaining Spiral Interlock

For interlocking spiral columns where shear is the dominant failure mode, individual spirals will tend to separate from one another under inelastic loading. In order to prevent spiral separation, an adequate number of longitudinal reinforcing bars must be placed within the interlock region. Tanaka and Park (2) and Caltrans (1) have proposed that at least four longitudinal bars should be placed in the

interlock region. Neither source lists a minimum requirement for the cross-sectional area of these interlock bars.

Shear Design

Tanaka and Park (2) have shown that the shear carried by the concrete in columns reinforced with interlocking spirals can be taken as

$$V_c = v_c b_w d$$

where v_c is the nominal shear stress carried by the concrete, b_w is the width of the column and

$$d = 0.5 b_w + d_{i1} + 0.318 D'$$

where d_{i1} is the distance between the centers of adjacent spirals and D' is the central diameter of the circular arrangement of longitudinal reinforcement.

Tanaka and Park (2) developed two methods for determining the shear carried by the interlocking spirals. The first method assumes that the overlapping portions of the spiral reinforcement do not reach yield stress due to ineffective interlock between the spirals, as shown in Figure 1a. Based on this assumption, the shear carried by the transverse reinforcement can be expressed as

$$V_s = \frac{\pi}{2} A_{sp} f_{yh} \frac{D'}{s} + 2 A_{sp} f_{yh} \frac{d_{i1}}{s}$$

where A_{sp} is the cross-sectional area of one spiral bar, f_{yh} is the yield stress of the spiral and s is the center-to-center spiral spacing. The second method assumes that all portions of the spiral reinforcement reach yield and are therefore effective against

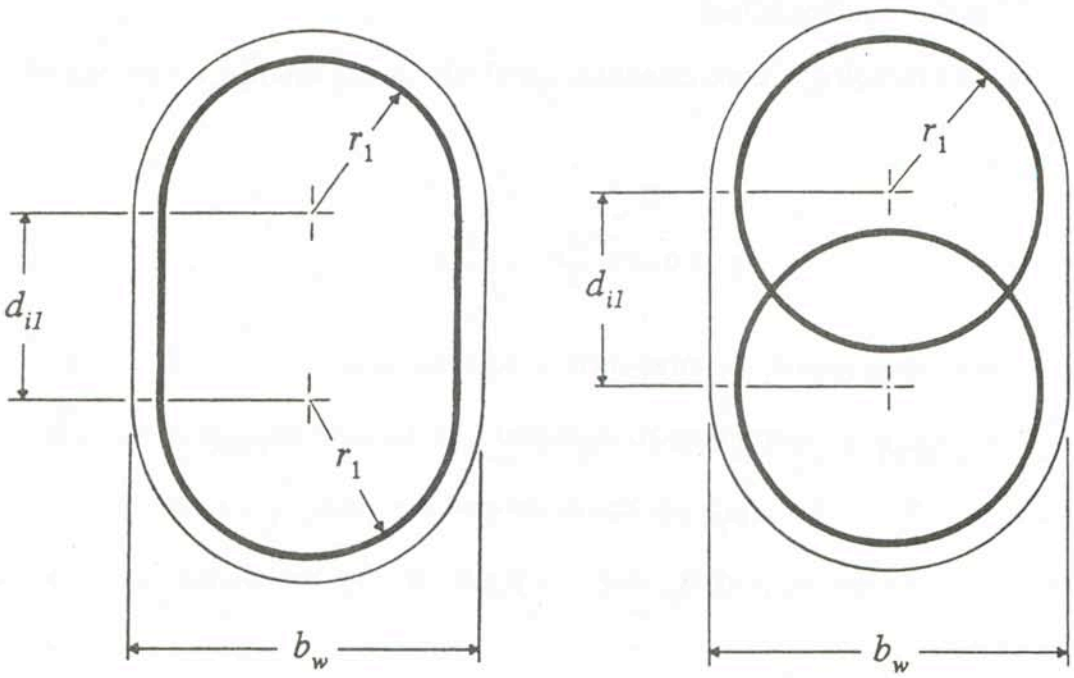

(a) (b)

Figure 1 Effective transverse reinforcement under shear loading.

shear, as shown in Figure 1b. The expression for shear carried by the transverse reinforcement can then be expressed as

$$V_s = \pi A_{sp} f_{yh} \frac{D'}{s}$$

which is equivalent to the shear resisted by two spiral columns.

Volume of Spiral Reinforcement

The ACI 318-89 (3) requirement for spiral reinforcing ratio (ρ_s) is expressed as

$$\rho_s = 0.45\left(\frac{A_g}{A_c} - 1\right)\frac{f'_c}{f_y}$$

where A_g is the gross area of the cross-section, A_c is the area of the spirally confined core, f'_c is the concrete compressive strength and f_y is the yield strength of the spiral reinforcement. Since this equation was developed for single spiral columns, the current definitions for A_g and A_c may not apply directly to interlocking spiral columns.

Tanaka and Park (2) recommend that the spiral reinforcement in interlocking spiral columns be designed as if for single equivalent spiral columns. The column is considered as individual spiral columns, with A_c being the area confined by a single spiral and A_g the area of an equivalent concrete cross-section concentric around a single spiral.

For plastic hinge detailing in interlocking spiral columns, Tanaka and Park (2) have shown that the current codified requirements for single spiral columns can be

applied to interlocking spiral columns using the assumptions described previously. Special detailing requirements for interlocking spiral columns with rectangular cross-sections have been addressed in the Caltrans Bridge Design Manual (4). Longitudinal bars are placed in the four corners of the column and outside both points of spiral intersection in order to minimize strength losses due spalling in these areas. The unconfined longitudinal bars are tied into the interlocking spiral core of the column using dead-ended anchors.

EXPERIMENTAL TESTS OF COLUMNS WITH INTERLOCKING SPIRALS

At the present time, the work done by Tanaka and Park (2) is the only information available on the experimental behavior of interlocking spiral columns. Tanaka and Park tested three interlocking spiral columns and one tied column under cyclic lateral load and constant axial load. The column specimens were designed to fail in flexure, and transverse reinforcement was provided in each column in accordance with the New Zealand Concrete Design Code (5) so as to develop plastic hinging at the column bases. Results of the tests showed similar levels of satisfactory performance for the tied column and the interlocking spiral columns, even though the tied column contained approximately 200% more transverse reinforcement by volume than the similar interlocking spiral column.

EXPERIMENTAL TESTING PROGRAM

TEST SPECIMENS AND PARAMETERS

Experimental tests were conducted on column specimens with both tied and interlocking spiral transverse reinforcement. The main tests were performed on eight approximately 1/5-scale column specimens subjected to cycled inelastic lateral displacements under constant axial load. Specimen details and test parameters were selected based on areas of design uncertainty and on results obtained from preliminary tests conducted on approximately 1/25-scale specimens. Details of the 1/25-scale study are given in reference 6.

Parameters investigated in the experimental testing program included the following: variation in spiral overlap percentage, the use of small-diameter (nominal) longitudinal reinforcement in the interlock zone, comparison of column performance with ties and interlocking spirals, variations in flexural detailing, and column cross-sectional shape. Cross-sections and reinforcement layout for the specimens investigated in the 1/5-scale study are shown in Figure 2. Details of the 1/5-scale testing program are summarized in Table 1. Additional information on the testing program can be found in reference 6.

The concrete used for all 1/5-scale specimens was typical of concrete used for bridge column construction. The concrete consisted of Type I/II Portland cement, river gravel coarse aggregate with a maximum size of 3/4 in., sand, water-reducer and an air-entraining agent. The average compressive strength at the time of testing was approximately 4600 psi.

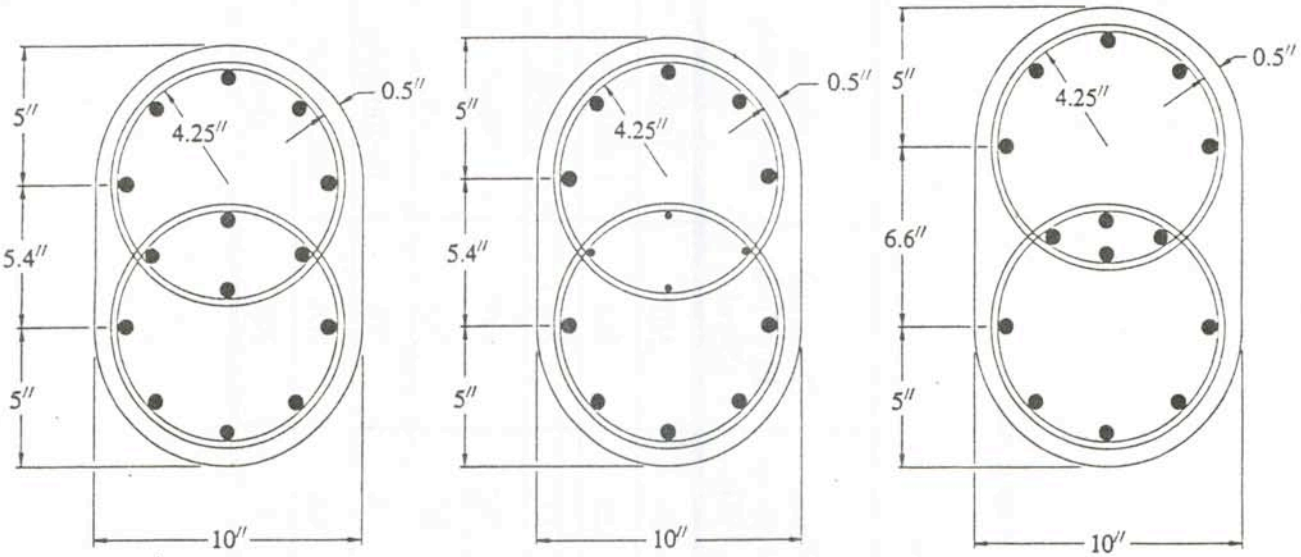

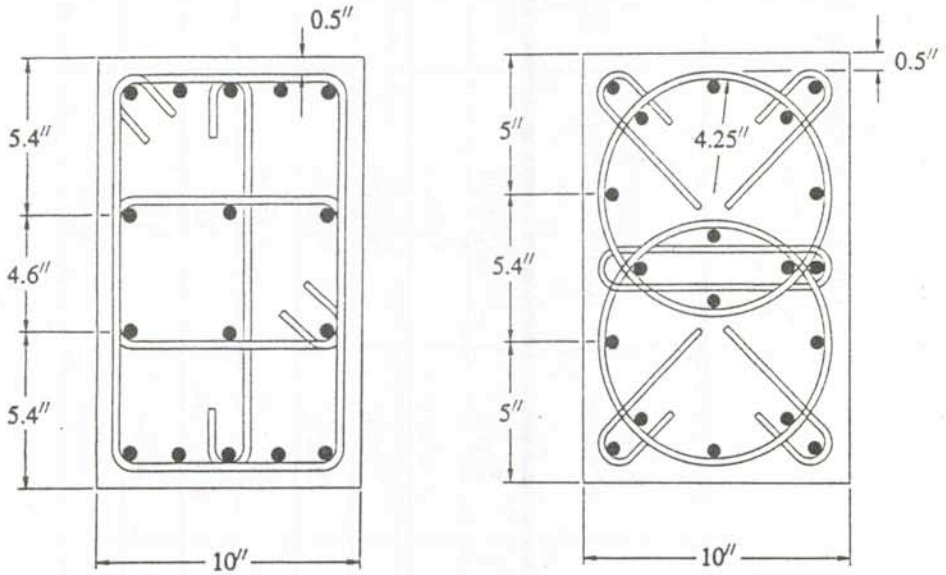

Figure 2 Column cross-sections and reinforcement layout.

Table 1 Parameters for 1/5-scale specimens.

Specimen Number	Type of Loading	Transverse Reinforcement	Spiral/Tie Spacing (in.)	Spiral Overlap (%)	Nominal Interlock Steel	Column Cross-section
1	Shear	Spirals	5.0	25	No	Oval
2	Flexural	Spirals	1.25	25	No	Rectangular
3	Shear	Spirals	5.0	15	No	Oval
4	Shear	Spirals	5.0	25	Yes	Oval
5	Flexural	Spirals	2.5	25	No	Oval
6	Flexural	Ties	2.5	NA	NA	Rectangular
7	Shear	Ties	5.0	NA	NA	Rectangular
8	Torsion	Spirals	5.0	25	No	Oval

All reinforcement in the 1/5-scale specimens was Grade 60. The ties and spirals were constructed of No. 2 deformed rebar. The column longitudinal steel consisted of No. 4 rebar in the flexural specimens and No. 5 rebar in the shear and torsion specimens, except for Column 4 which had No. 2 rebar in the interlock zone.

TEST SETUP AND PROCEDURES

The test setup for the 1/5-scale shear and flexure specimens is shown in Figure 3. The footing of the test specimen was anchored to a laboratory strong floor. Lateral load was applied using a 55-kip actuator operated under displacement control. Axial load was applied to the top of the column using a 200-kip jack. An axial load of approximately 0.09 $f'_c A_g$ was applied to all specimens except that used in the torsion test, which had no axial load. The axial loading system resulted in the axial load varying during testing by approximately ±6%.

The method for determining the yield displacement for the 1/5-scale specimens is illustrated in Figure 4. The theoretical ACI ultimate moment strength (M_{ACI}) of each column was determined using strain compatibility methods. The column was then subjected to ±75% M_{ACI} under load control and the corresponding deflections of $\pm\Delta_e$ were recorded. The yield displacement (Δ_y) was determined using the equation shown in Figure 4. The specimens were subjected to a simulated seismic loading pattern consisting of increasing multiples of Δ_y in order to demonstrate the ductility and hysteretic behavior of the test specimens. The loading pattern for the flexure specimens consisted of two cycles at displacement ductility

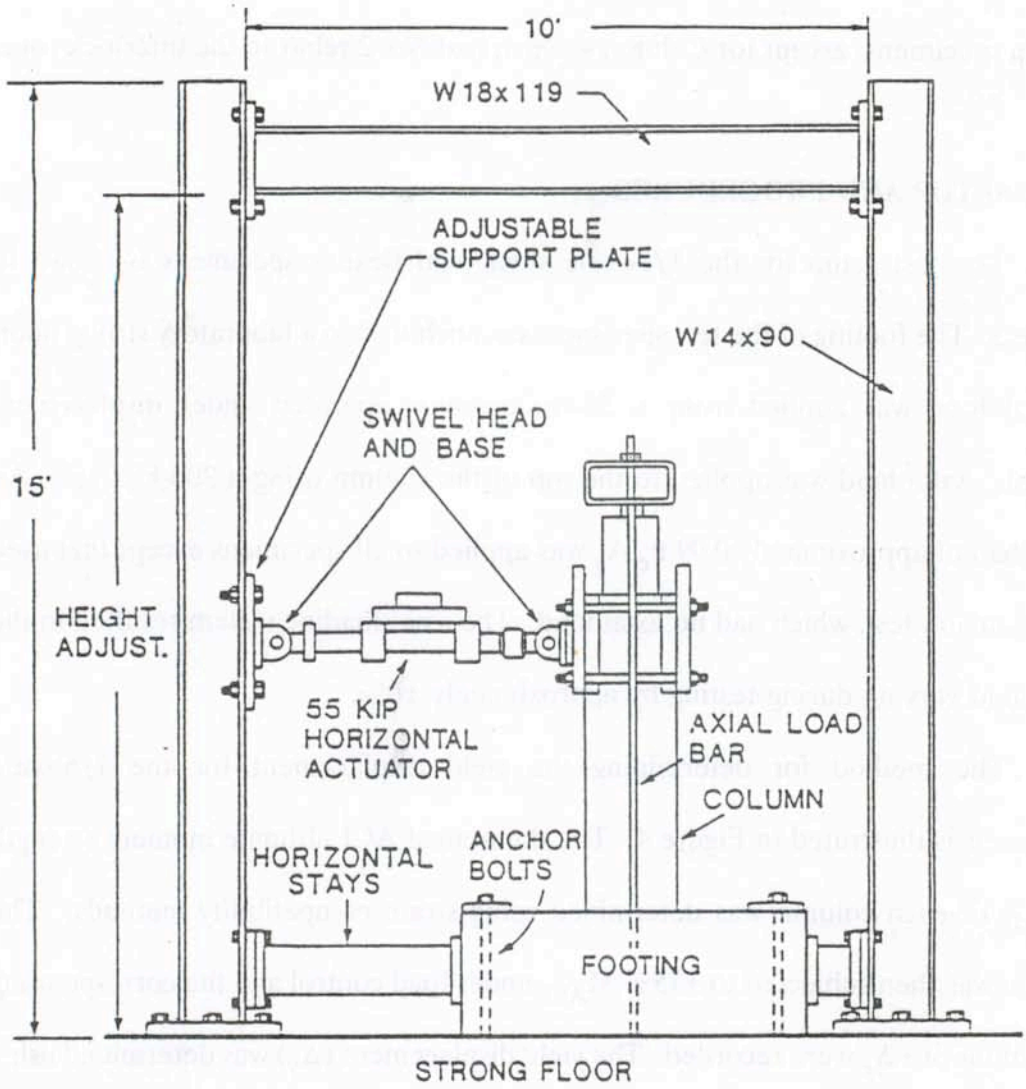

Figure 3 Test setup.

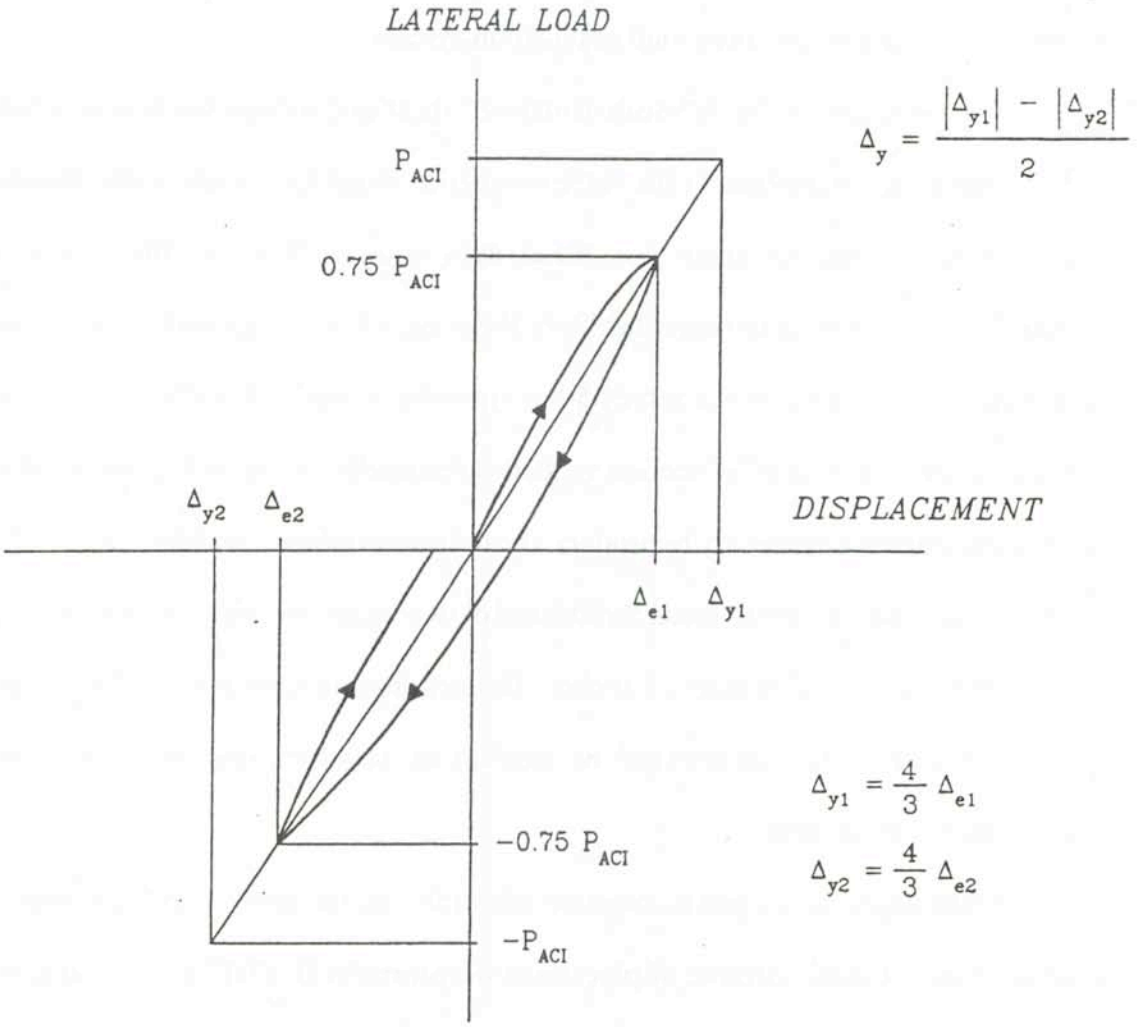

Figure 4 Determination of specimen yield displacement.

levels (i.e. multiple values of Δ_y) of $\mu = \pm 1, \pm 2, \pm 4, \pm 6$, and ± 8, with the exception of Column 2, which was taken to a maximum displacement level of $\mu \approx \pm 7$ due to actuator stroke limitations. The loading pattern for the shear test specimens was halted at a displacement ductility level $\mu = \pm 4$ due to failure of the specimen and possible instability of the axial load application system.

The specimen for the 1/5-scale combined shear and torsion test was attached to the laboratory strong floor in the same manner as those for the shear and flexure tests. However, the specimen was offset approximately 6 in. in the direction perpendicular to loading to better facilitate the eccentric loading system. Load was applied to the column with the same 55-kip hydraulic actuator described earlier. A loading collar with a steel W-section welded horizontally to one side provided the eccentric connection necessary to produce the desired combined loading effect. The load sequence used to test Column 8 consisted of two cycles at displacements of ±0.5, ±1.0, ±1.5, ±2.0, ±2.5, ±3.0 and ±3.5 inches. Deflections and loads recorded from the 55-kip actuator were transformed to equivalent rotations and torques using trigonometric relationships.

Strain gages were used to monitor the strains in the flexural and transverse reinforcement. Linear variable displacement transformers (LVDT's) and load cells measured column displacements and applied loads. All data was recorded intermittently during testing.

TEST RESULTS AND DISCUSSION

SHEAR TESTS

General Behavior

Column 1 was an interlocking spiral column with the minimum overlap percentage of 25 recommended by Tanaka and Park (2) and full-size longitudinal bars in the interlock zone. Test results from this specimen were used as a guideline for comparison to the other shear tests. Initial cracking occurred at a lateral load of approximately 20 kips. An x-crack pattern typical of shear deficient reinforced concrete columns under cycled inelastic displacements formed at $\mu = \pm 1$, and crack widths increased at $\mu = \pm 2$. A photograph of the crack patterns exhibited in Column 1 at $\mu = \pm 2$ is shown in Figure 5a. Cracking in the specimen eventually led to spalling of the cover concrete and internal fragmentation of the core at $\mu = \pm 4$. Damage to the reinforcing steel at this final displacement level was limited to straightening of the spiral between longitudinal bars, as shown in Figure 5b. The load-displacement curve for Column 1 is shown in Figure 6a. The load-carrying capacity of the specimen remains virtually constant at $\mu = \pm 1$ and displays a small decrease at $\mu = \pm 2$. However, severe degradations in lateral load capacity corresponding to the physical damage mentioned earlier are apparent at $\mu = \pm 4$.

Column 4 was designed in the same manner as Column 1 with the exception of the smaller longitudinal bars (No. 2 rebar) in the interlock zone. The initial cracking load for Column 4 was approximately 22 kips. The x-crack pattern displayed in Column 1 was also apparent in this specimen for displacement levels of $\mu \leq \pm 2$.

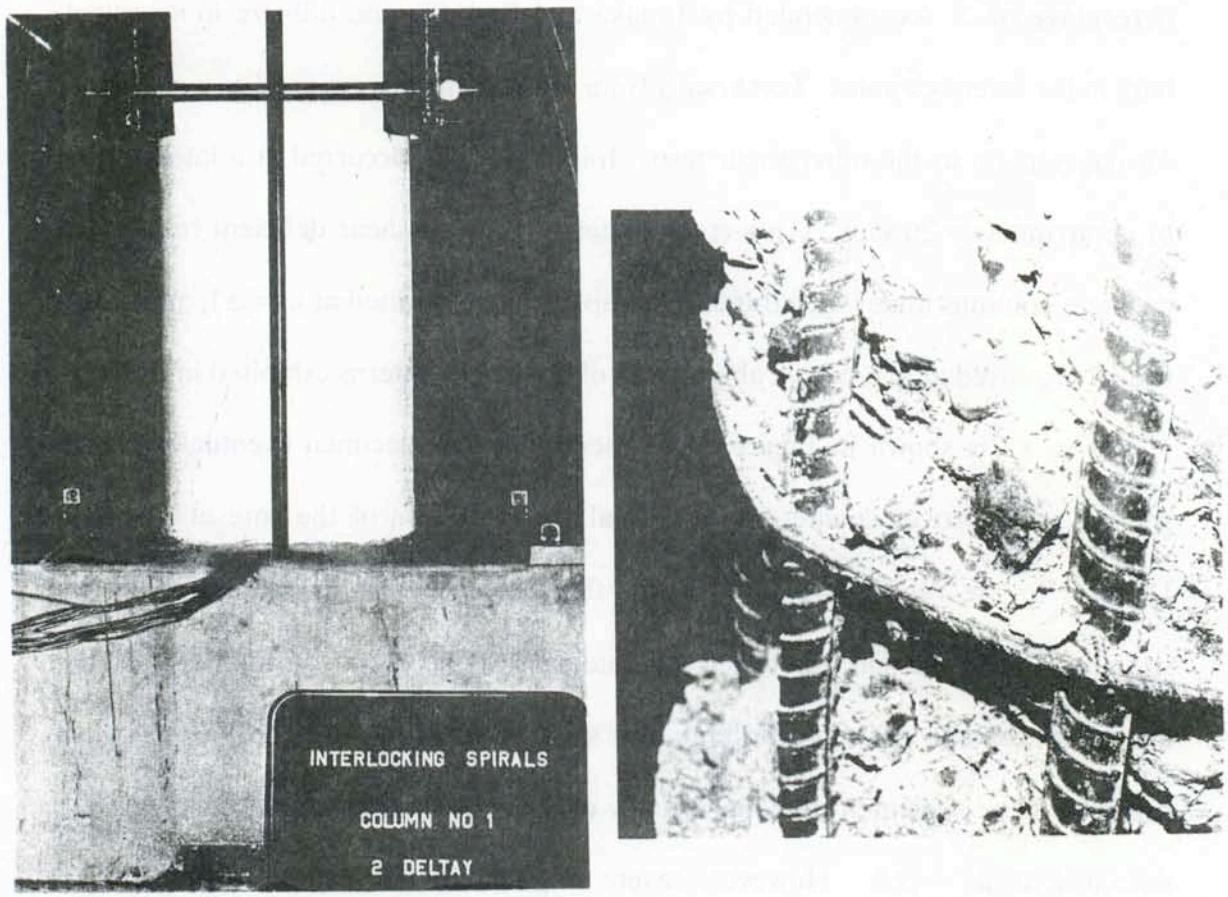

(a) (b)

Figure 5 Photographs of Column 1 showing (a) crack patterns at $\mu = \pm 2$ and (b) spiral straightening during testing.

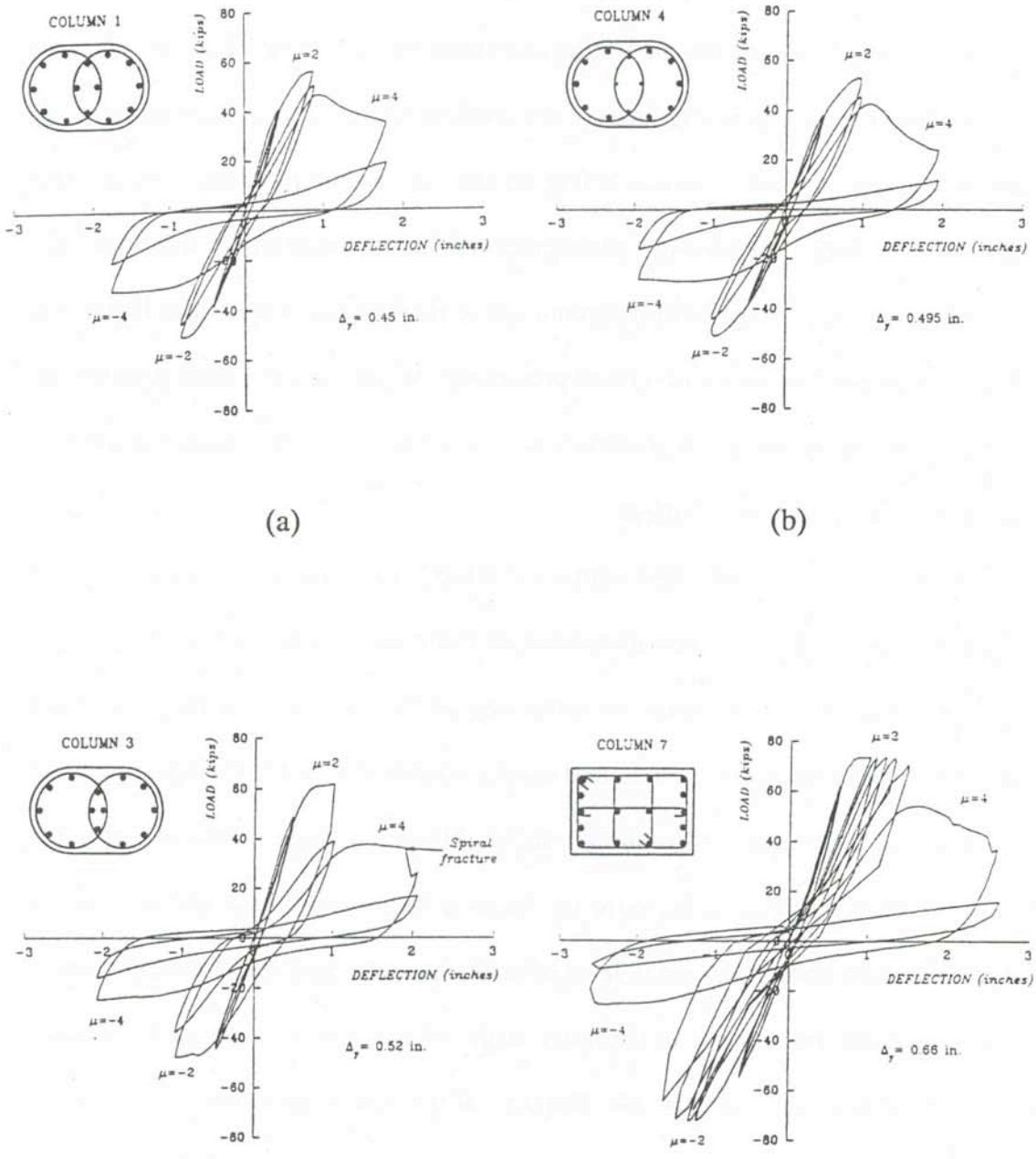

Figure 6 Load-displacement curves for the shear test specimens.

However, the crack widths in Column 4 were larger than those in Column 1 at μ = ±2, as shown in Figure 7a. Spalling of the cover concrete started early in the μ = ±4 cycle, followed by core fragmentation and spiral straightening. The two nominal interlock bars on the transverse faces of the column displayed significant amounts of deformation due to tensile forces acting on the spiral reinforcement arising from shear on the column. A post-test photograph of one of the nominal interlock bars is shown in Figure 7b. The load-deflection curve for Column 4, shown in Figure 6b, reflects the physical behavior described previously. Moderate degradation occurs for $\mu \leq \pm 2$, followed by severe degradation at $\mu = \pm 4$ due to core fragmentation and longitudinal reinforcement damage.

Column 3 was constructed with an overlap percentage of 15 to examine the minimum overlap of 14.3% recommended by Caltrans (1). All of the longitudinal bars in the interlock zone were the same size as the bars used in the rest of the specimen. The initial cracking load and crack pattern exhibited in this specimen was similar to that described for Columns 1 and 4. However, crack widths in Column 3 at $\mu = \pm 2$, shown in Figure 8a, were significantly larger than those encountered in the previous two tests at the same level of displacement. Spalling of cover concrete in this specimen commenced in the latter stages of the $\mu = \pm 2$ cycle and continued into the final two cycles at $\mu = \pm 4$. Rupture of the spiral reinforcement, shown in Figure 8b, occurred on the first cycle to $\mu = +4$ at approximately 93% of full cycle displacement. The load-deflection plot for Column 3 is shown in Figure 6c. Decreases in the load carrying capacity of the column are detectable at every level

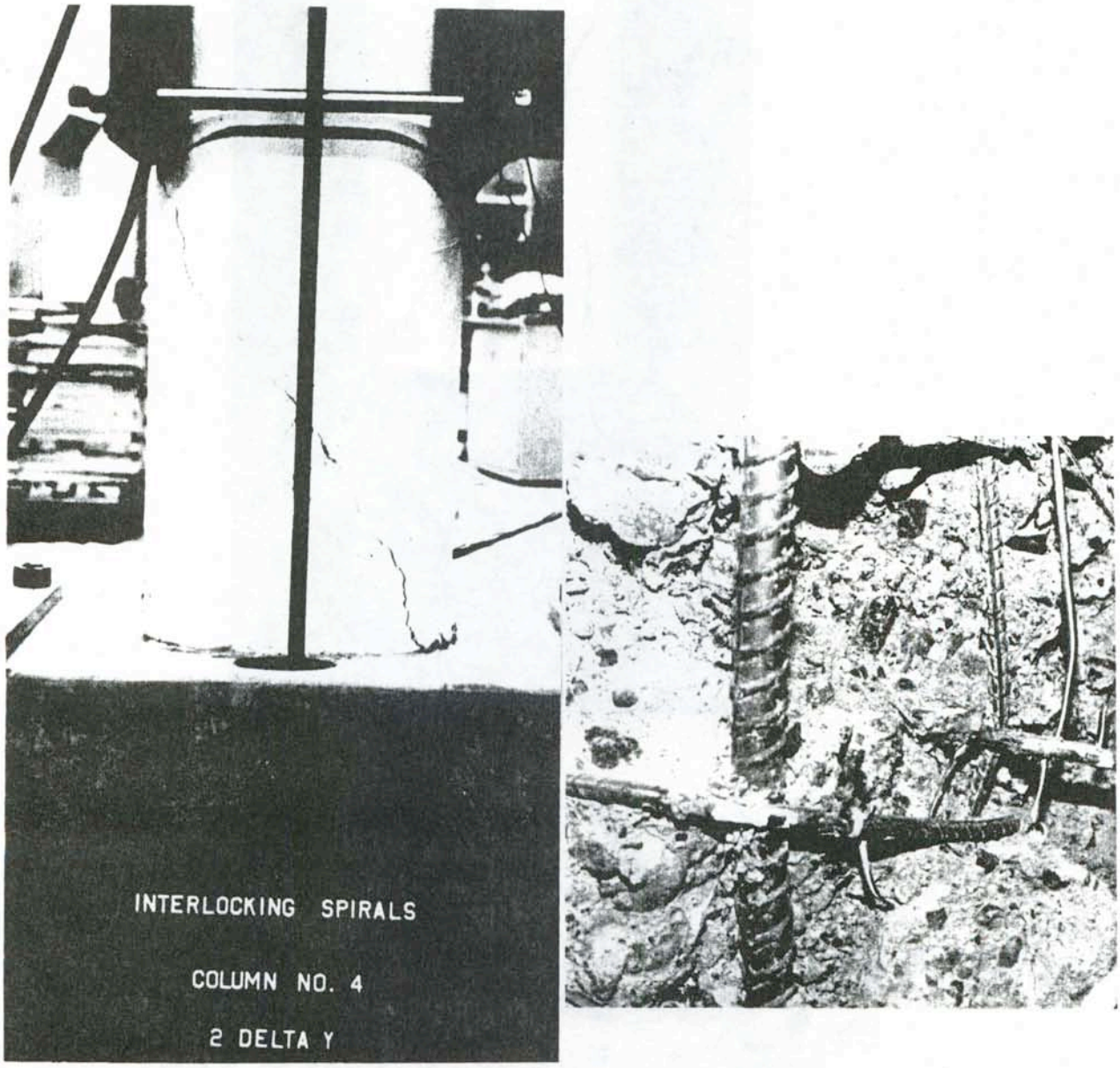

(a) (b)

Figure 7 Photographs of Column 4 showing (a) crack patterns at $\mu = \pm 2$ and (b) nominal interlock bar after testing.

(a)

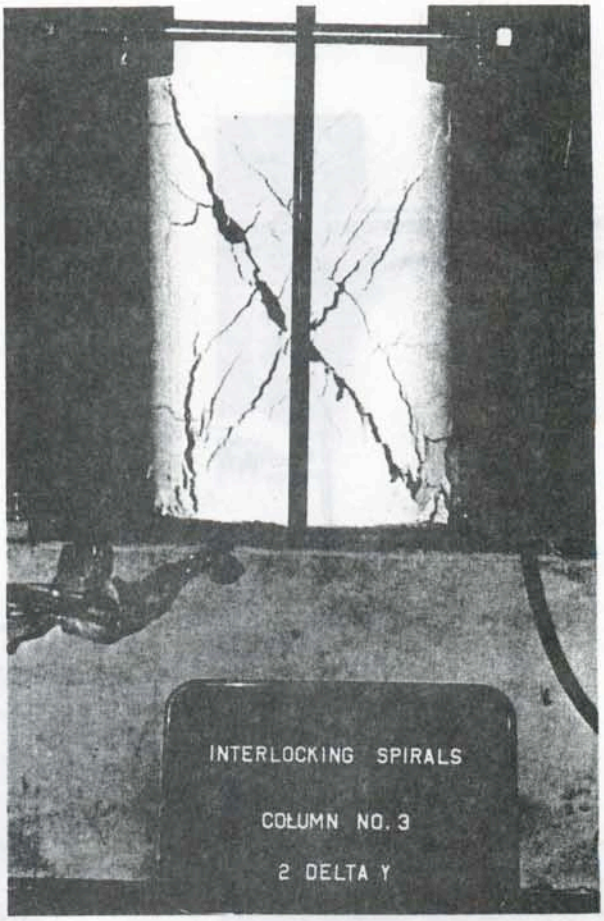

(b)

Figure 8 Photographs of Column 3 showing (a) crack patterns at $\mu = \pm 2$ and (b) rupture of the spiral reinforcement.

of displacement ductility past the first cycle to $\mu = +2$. The fracture point of the spiral reinforcement is indicated by the near vertical drop in lateral load on the first cycle to $\mu = +4$.

Rectangular ties and cross-ties were used as transverse reinforcement in Column 7 in order to compare the performance of a conventionally reinforced column to one utilizing the interlocking spiral detail (Column 1). A modified testing procedure was used for Column 7 due to limitations encountered in the capacity of the testing equipment. The first two cycles at $\mu = \pm 1$ were accomplished without any alterations to the testing procedure or equipment. However, the load required to attain a displacement corresponding to $\mu = \pm 2$ was beyond the range of the 55-kip hydraulic actuator. After two failed attempts to reach $\mu = +2$ with normal testing procedures, the specimen was relieved of all axial load and cycled manually to produce strength deterioration until the desired displacement was obtained. A photograph showing crack patterns at $\mu = \pm 2$ is shown in Figure 9a. For the cycle to $\mu = \pm 4$, axial load was returned to the specimen and normal procedures for controlling the lateral load and displacement were resumed. Degradation of Column 7 occurred rapidly in the final two cycles at $\mu = \pm 4$. The core concrete was reduced to rubble at this stage due to the loss of confinement, and possibly also due to the increased number of load cycles imposed on this specimen. A post-test photograph of one of the rectangular ties in Column 7 is shown in Figure 9b. The bend angle on the end return has rotated from an original position of 135 degrees to approximately 90 degrees, resulting in a partial loss of the confinement capability of

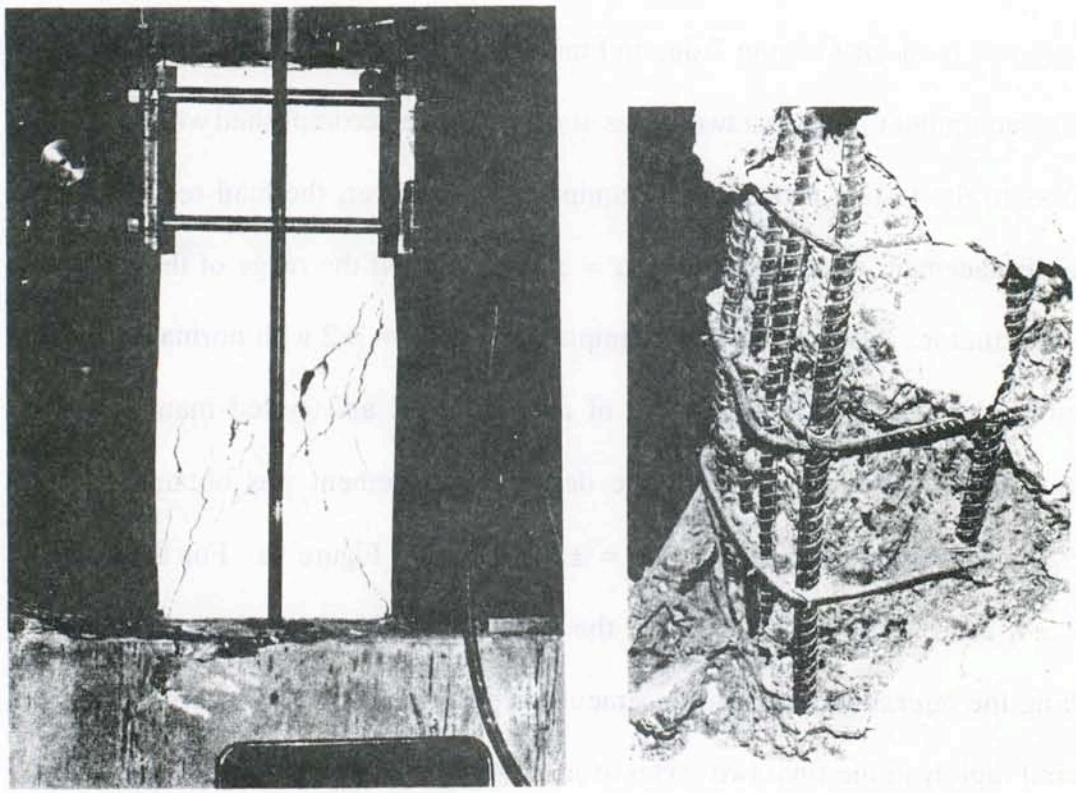

(a) (b)

Figure 9 Photographs of Column 7 showing (a) crack patterns at $\mu = \pm 2$ and (b) the rectangular tie end returns after testing.

the tie. Similar damage to the end returns on the internal ties and cross-ties also occurred. The load deflection plot for Column 7 is shown in Figure 6d. Although influenced by the increased number of cycles used at $\mu = \pm 2$, the graph reveals rapid deterioration in the load carrying capacity of the specimen at $\mu = \pm 4$, as described earlier. The two sharp drops in load at deflections of approximately 2.0 in. and 2.5 in. on the first cycle to $\mu = \pm 4$ correspond to sudden unraveling of rectangular tie end returns.

Comparison of Hysteresis Curves

A graph displaying load-deflection envelope curves for each of the four 1/5-scale shear test specimens is shown in Figure 10. Points on the graph represent the peak load carried by each specimen at successive levels of displacement ductility, μ. By representing the data in this manner, it is possible to directly compare the degradation characteristics inherent to each column. Comparison of the load-deflection data indicates that the reduction in load carrying capacity for Columns 3 and 4 was greater than that for Column 1 at similar levels of displacement ductility. The load-deflection envelope curve for Column 7 reveals a degradation in load carrying capacity that is comparable to that in Columns 3 and 4 and is significantly greater than the degradation in Column 1. However, it is important to note that the testing procedure used for Column 7 was different from that used in the rest of the tests.

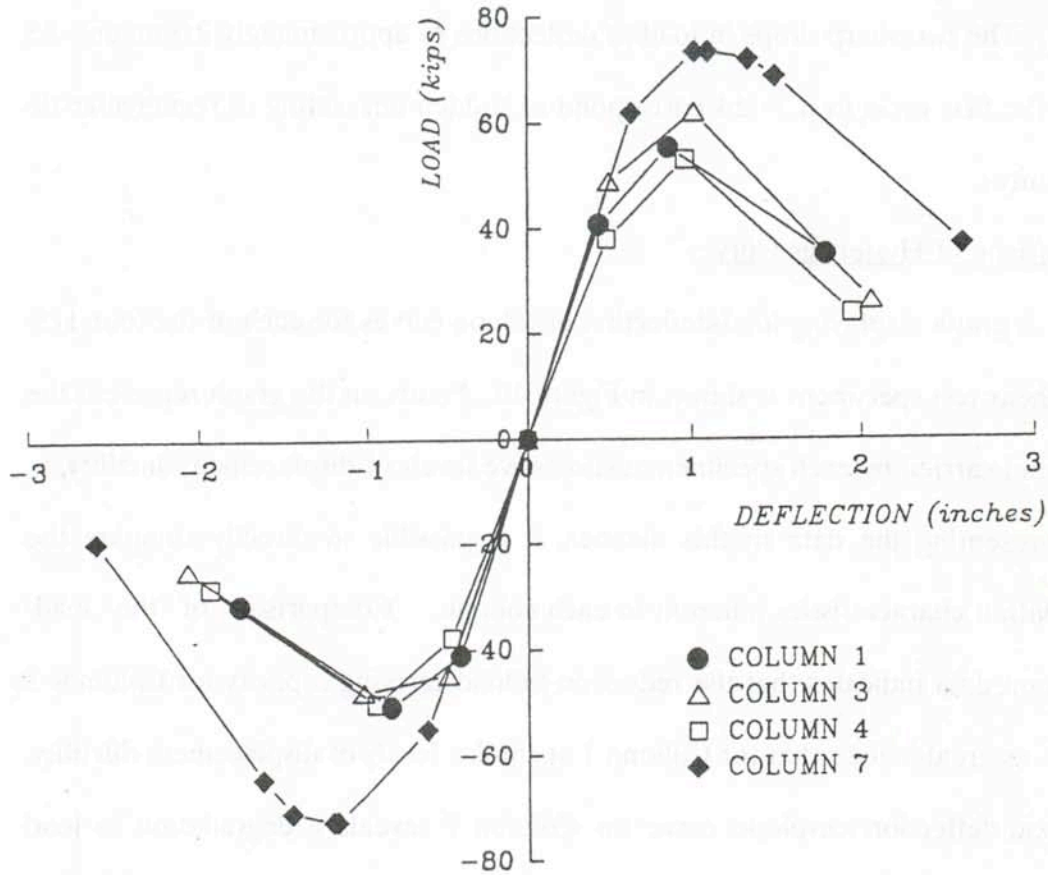

Figure 10 Lateral load-deflection envelope curves for the shear test specimens.

Comparison of Energy Dissipation Characteristics

A definition of energy dissipation is outlined in Figure 11. The area enclosed by an experimental load-deflection curve (E) for a structural member is equal to the energy dissipated in the member through inelastic displacements. When this value is divided by the area enclosed by an idealized elastic-plastic member (E_p), the result is an efficiency factor for energy dissipation in that particular member (E_r). A plot of energy dissipation ratio, E_r, versus displacement ductility factor, μ, for Columns 1, 3 and 4 is shown in Figure 12. Comparison of this data reveals that Column 1 is slightly more efficient than Column 3 and significantly higher in efficiency than Column 4 with respect to energy dissipation. Data for Column 7 was not included in Figure 15 due to the difference in testing procedure.

Comparison of Calculated and Experimental Strengths

A summary of the experimental and theoretical ultimate shear strengths for the 1/5-scale shear test specimens is shown in Table 2. The theoretical shear strengths for interlocking spiral columns were calculated based on the procedures developed by Tanaka and Park (2) and assuming that the spiral reinforcement was fully effective. The ratios of experimental to theoretical shear strength for the interlocking spiral columns (Columns 1, 3 and 4) are all within 4.4% of one another. This difference is negligible considering the inconsistent nature of shear failure in reinforced concrete members. The normalized shear strength for Column 7 also falls within the range of scatter established by the other shear specimens. The calculated shear strength for Column 7 was determined assuming all portions of the outer ties,

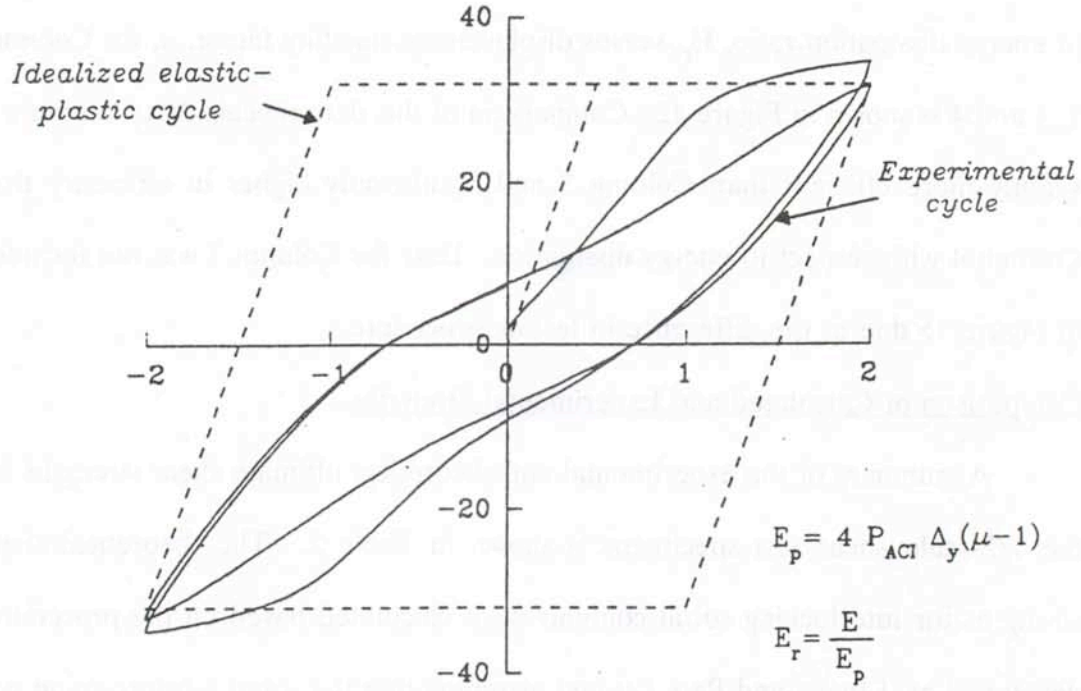

Figure 11 Definition of energy dissipation ratio, E_r.

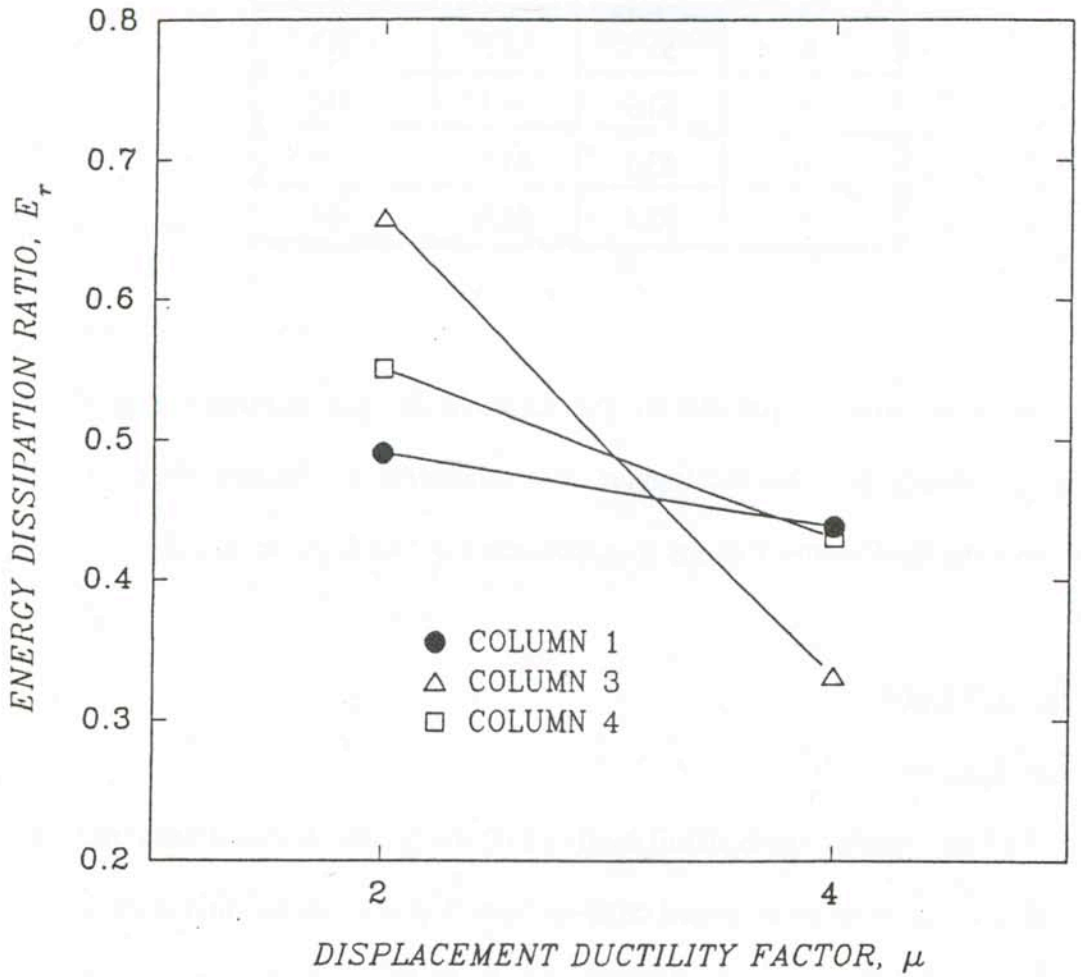

Figure 12 Energy dissipation ratio versus displacement ductility for shear specimens.

Table 2 Summary of 1/5-scale shear test results.

Specimen Number	V_{test} (kips)	V_n (kips)	$\frac{V_{test}}{V_n}$
1	55.5	41.2	1.347
3	61.9	44.5	1.391
4	53.1	38.5	1.379
7	73.4	53.8	1.364

inner ties and cross-ties parallel to the direction of load contributed to shear resistance. If only the outer rectangular tie is considered as effective, the predicted shear strength for Column 7 drops by approximately 14.2-kips, or 26.4%.

FLEXURE TESTS

General Behavior

The interlocking spiral detail used in Column 5 consisted of a spiral overlap percentage of 25 in an oval-shaped cross-section. Flexure cracks initially appeared in Column 5 at a lateral load of approximately 15 kips. At $\mu = \pm 1$, shear and flexure-shear cracks formed along the entire height of the specimen at intervals of approximately 3 in. to 4 in. Although these cracks persisted throughout the duration of the test, the primary mode of failure in the specimen remained flexural in nature. Crushing of the concrete on the extreme load-bearing faces of the specimen just

above the top of the footing occurred at $\mu = \pm 4$ and eventually led to spalling in these areas at $\mu = \pm 6$, as shown in Figure 13a. On the final cycle to $\mu = +6$, the longitudinal bar shown in Figure 13b buckled outward between two sections of spiral reinforcement. Further cycling of the specimen resulted in fracture of this bar at $\mu = -8$ due to fatigue stress. The load-displacement curve for Column 5 is shown in Figure 14a. Except for the sharp drop in lateral load at the point of longitudinal bar fracture, the load carrying capacity of the specimen remains nearly constant throughout the test.

Column 6 represented a conventionally designed reinforced concrete column with rectangular ties and cross-ties used as transverse reinforcement. The initial cracking load for Column 6 was approximately 13-kips. Crack patterns and crack development for this specimen were similar to those in Column 5 for $\mu \leq \pm 2$. Spalling of the cover concrete on both of the extreme compression faces began at $\mu = \pm 4$ due to minor buckling of the longitudinal reinforcement. The lack of confinement from the rectangular ties and cross-ties led to severe buckling of the longitudinal reinforcement and unraveling of tie and cross-tie end returns at $\mu = \pm 6$, as shown in Figure 15. Continued cycling through $\mu = \pm 8$ resulted in the fracture of five of the ten longitudinal reinforcing bars concentrated on each of the short faces of the column. The load-deflection plot for Column 6 is shown in Figure 14b. The load carrying capacity of the specimen remains stable for $\mu \leq \pm 6$, then drops significantly at $\mu = \pm 8$ due to fracture of the longitudinal reinforcement.

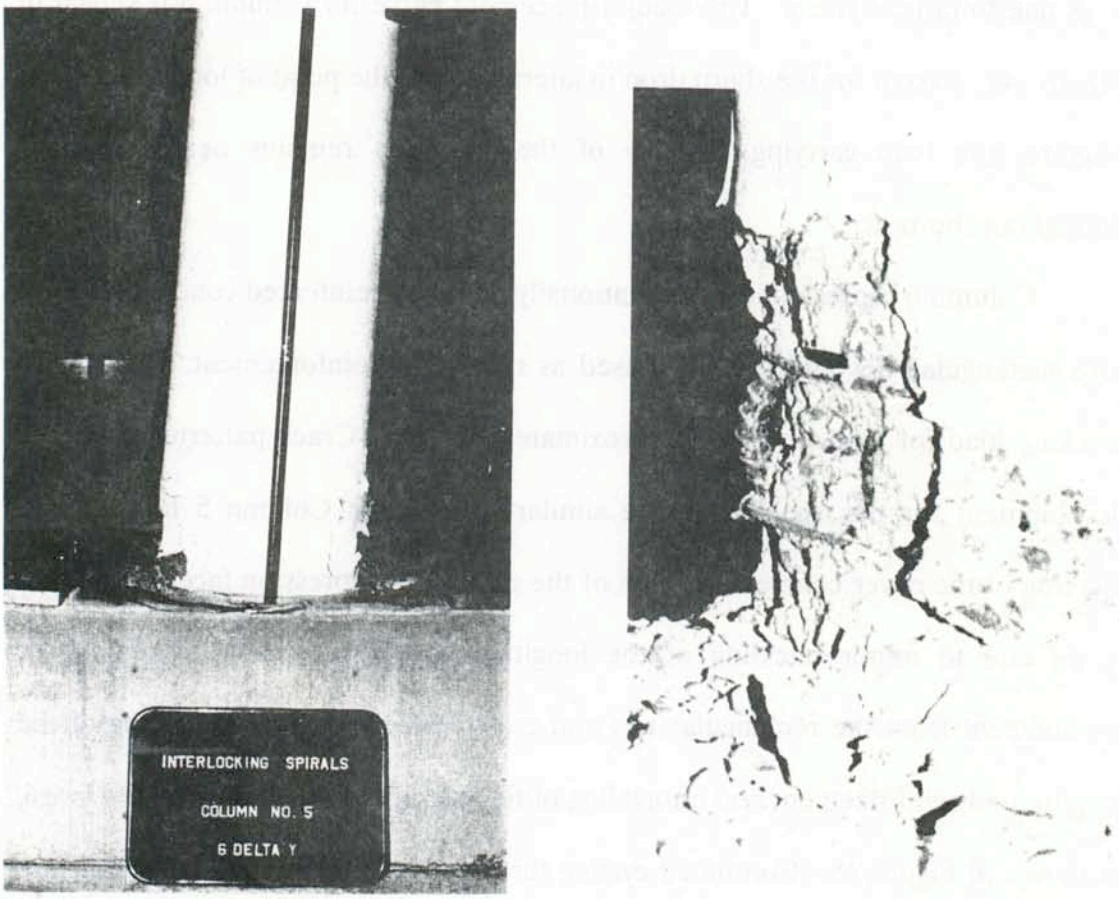

(a) (b)

Figure 13 Photographs of Column 5 showing (a) damage at $\mu = \pm 6$ and (b) buckling of the longitudinal reinforcement.

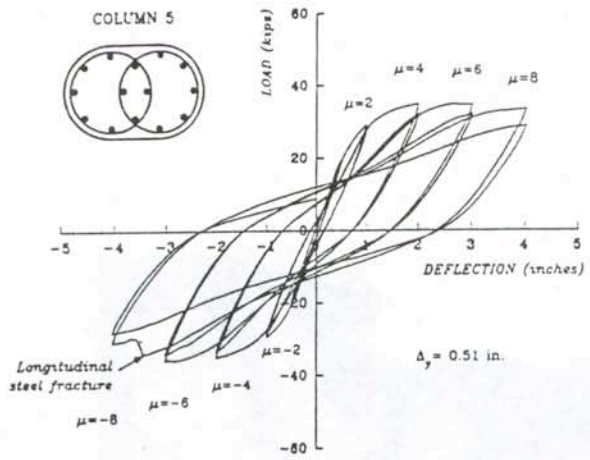

(a)

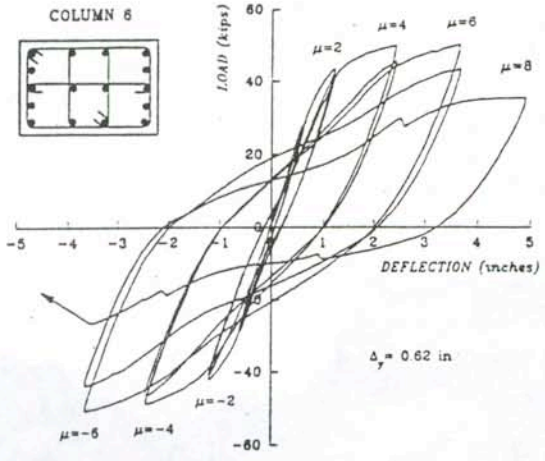

(b)

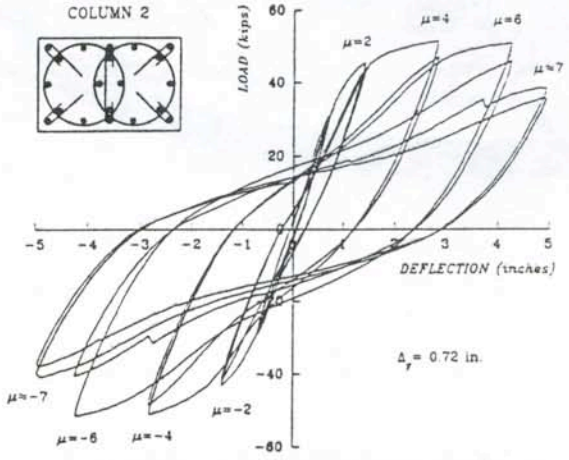

(c)

Figure 14 Load-displacement curves for the flexural test specimens.

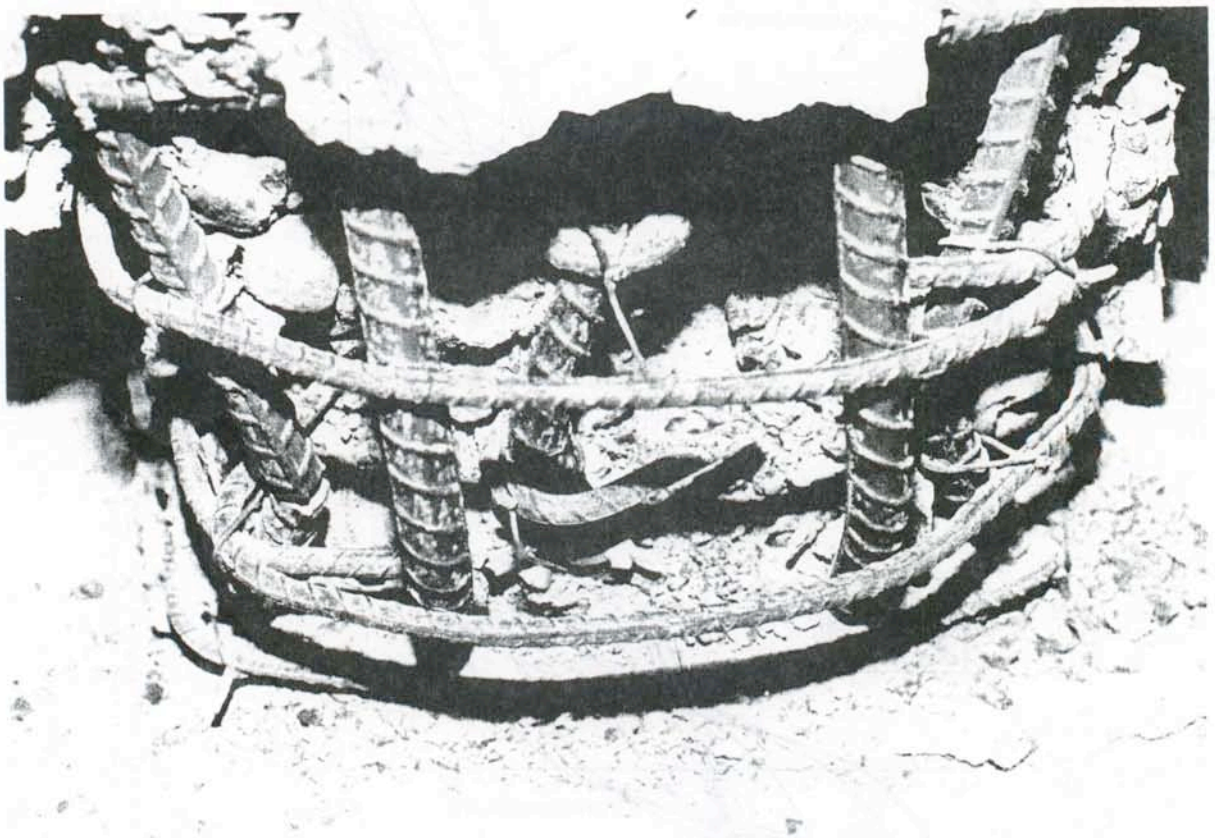

Figure 15 Buckling of the longitudinal reinforcement in Column 6.

Column 2 was constructed to investigate a reinforcing detail used for interlocking spiral columns enclosed in rectangular concrete cross-sections. The cracking pattern in Column 2 for $\mu \leq \pm 2$ was similar to that described for Column 5. Deterioration of the cover concrete commenced at $\mu = \pm 4$, along with moderate buckling of the four unconfined corner longitudinal bars. Cycles to $\mu = \pm 6$ and $\mu \approx \pm 7$ led to the fracture of all four unconfined corner bars, moderate buckling of the confined longitudinal bar on the extreme bending face and necking of the spiral reinforcement. The load-deflection plot for Column 2 is shown in Figure 14c. The load carrying capacity of the specimen shows little degradation through $\mu = \pm 4$, then drops sharply during loading to $\mu = \pm 6$ and $\mu \approx \pm 7$ due to longitudinal bar fracture.

Comparison of Hysteresis Loops

The load-deflection envelope curves for all of the 1/5-scale flexure specimens are shown in Figure 16. The degradation in peak load carrying capacity for Column 5 from $\mu = +4$ to $\mu = +8$ is 1.4 kips or 4.0%. In comparison, the capacity of Column 6 increases slightly through $\mu = \pm 6$, then drops 14.6 kips or 29.1% at $\mu = \pm 8$. This data indicates that Column 5 maintained a higher percentage of peak load than Column 6 at similar levels of displacement ductility. The degradation in load carrying capacity for Column 2 from $\mu = +4$ to $\mu \approx +7$ is 13.2 kips, or 25.6%, and is primarily the result of unconfined longitudinal bar fracture.

Comparison of Energy Dissipation Characteristics

A plot of energy dissipation ratio, E_r, versus μ for Columns 2, 5 and 6 is shown in Figure 17. The energy dissipation of Column 5 increases at each successive

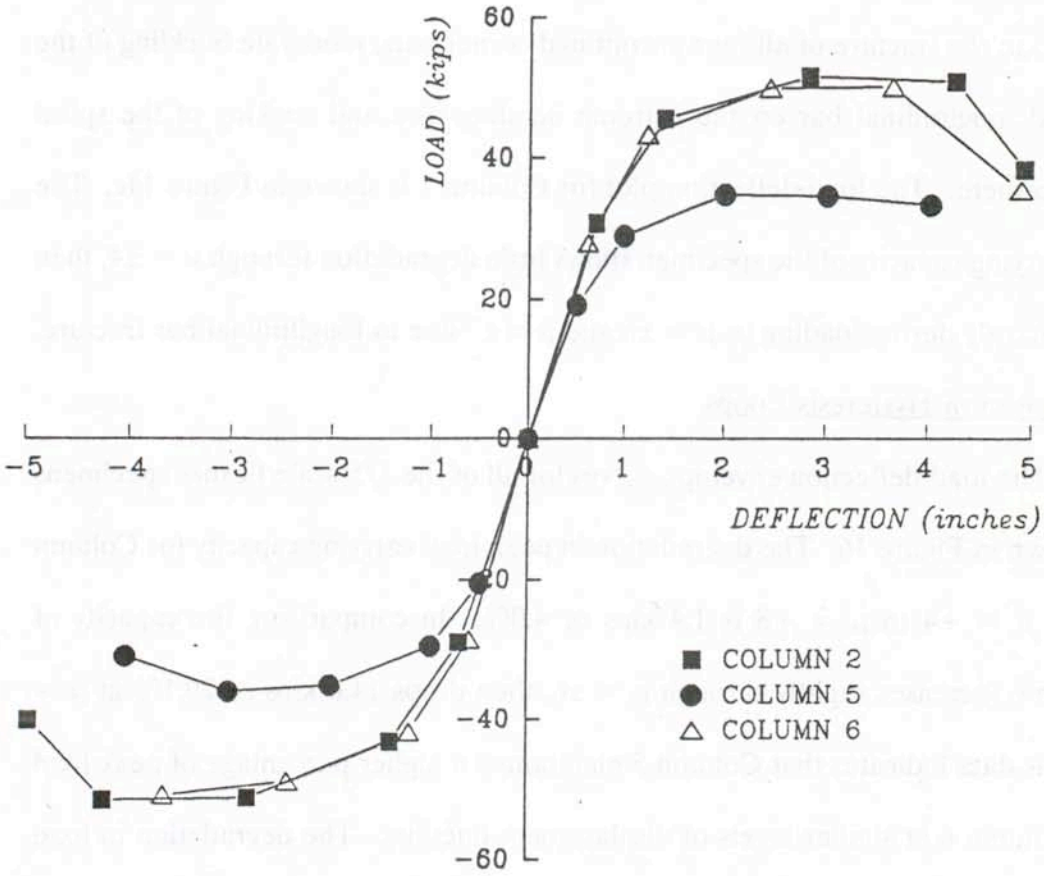

Figure 16 Lateral load-deflection envelope curves for flexural test specimens.

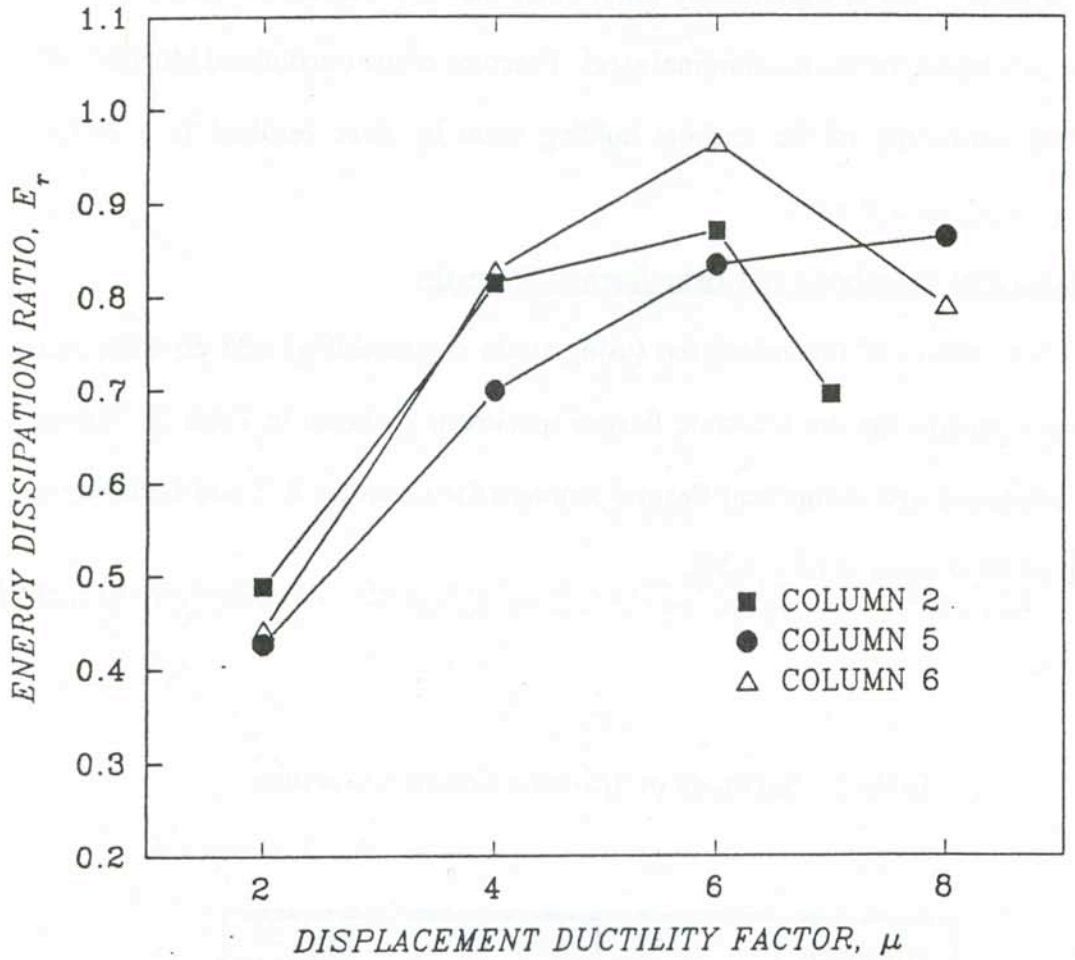

Figure 17 Energy dissipation ratio versus displacement ductility for flexure specimens.

level of μ, while Column 6 displays a decrease of 18.1% from $\mu = \pm 6$ to $\mu = \pm 8$. A comparison of the two specimens indicates that Column 5 is more efficient than Column 6 with respect to energy dissipation. The increase in E_r for Column 2 from $\mu = \pm 4$ to $\mu = \pm 6$ is significantly lower than that for Columns 5 and 6 due to advanced buckling of the longitudinal steel. Fracture of the unconfined longitudinal bars and unraveling of the anchors holding them in place resulted in a 20.1% decrease in E_r at $\mu \approx \pm 7$.

Comparison of Calculated and Experimental Strengths

A summary of the calculated (using strain compatibility) and experimental ultimate strengths for the 1/5-scale flexure specimens is shown in Table 3. Ratios of experimental and theoretical flexural strength for Columns 2, 5 and 6 display a maximum difference of only 4.2%.

Table 3 Summary of 1/5-scale flexure test results.

Specimen Number	M_{test} (in.-kips)	M_{ACI} (in.-kips)	$\frac{M_{test}}{M_{ACI}}$
2	2,477	1,913	1.295
5	1,723	1,291	1.335
6	2,438	1,824	1.337

COMBINED SHEAR AND TORSION TEST

General Behavior

Column 8 was an exact replica of Column 1, with an overlap percentage of 25 and an oval-shaped cross-section. The purpose of this test was to investigate the ultimate state behavior of an interlocking spiral column under combined shear and torsional load. Initial cracking in Column 8 occurred at a torsional load of approximately 110 in.-kips. A spiral cracking pattern was exhibited in the specimen and was typical of cracking in reinforced concrete members under combined shear and torsional load. Cracking became more severe at $\Delta = \pm 1.0$ in. (approximately ±2.88-degree rotation) and was followed by spalling of the cover concrete at $\Delta = \pm 1.5$ in. (approximately ±4.3-degree rotation). Additional cycles resulted in straightening of the spiral reinforcement around the longitudinal bars and some internal cracking of the concrete core.

The torque-twist curve for Column 8 is shown in Figure 18. The data displayed in the graph includes corrections for rotations in the loading collar and actuator and translations parallel and perpendicular to the plane of the reaction frame. The most prominent characteristic depicted in this graph is the difference in specimen degradation at positive and negative values of rotation. For positive values of rotation, the degradation in peak torque-carrying capacity for Column 8 is approximately 47%. In contrast, the deterioration in the capacity of the specimen for negative values of rotation is only 12%.

A possible explanation for this phenomena is the fact that spiral reinforcement

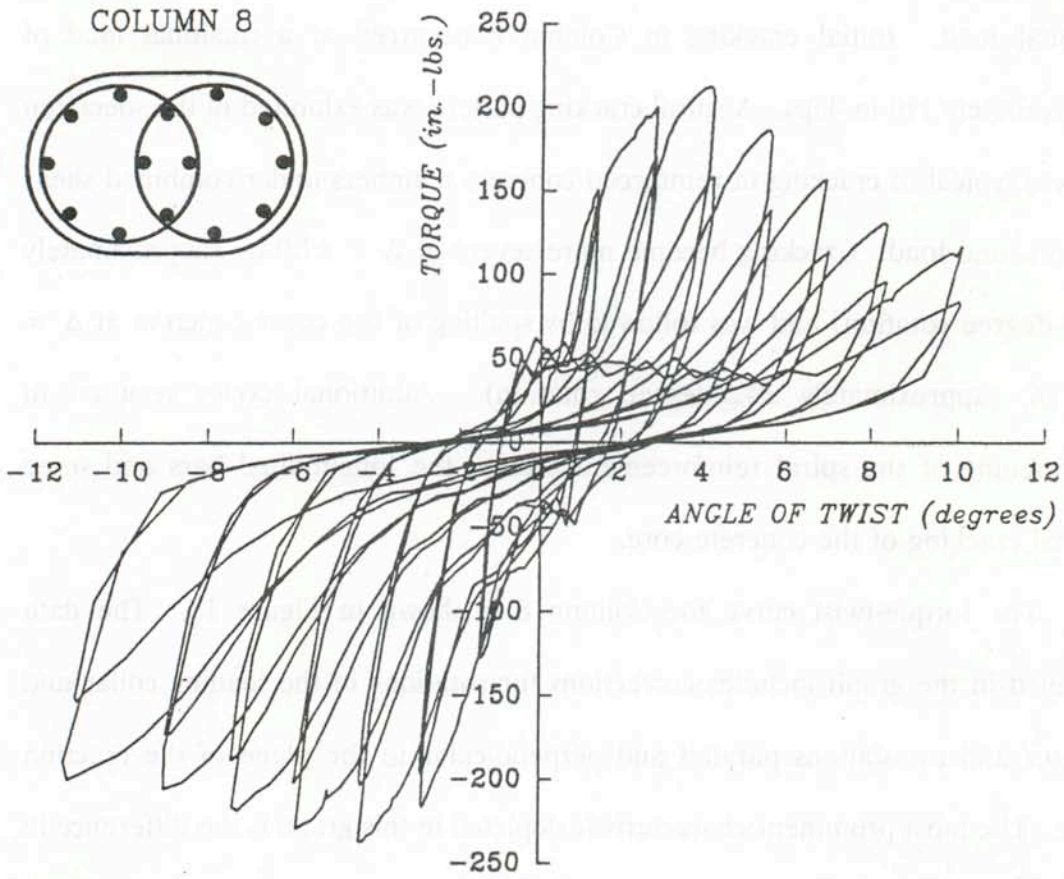

Figure 18 Torque-twist curve for Column 8.

tends to tighten around the concrete core when twisted in one direction and separate from the core when twisted the opposite direction. The orientation of the spirals is Column 8 were such that a twist in the clockwise direction (negative rotation on the graph) resulted in tightening of the spiral, while a counter-clockwise twist (positive rotation on the graph) resulted in unwinding of the spiral. Strain gage readings on the spiral reinforcement and visual observation of separation of the spiral reinforcement from the concrete core during counter-clockwise loading supports this hypothesis of an winding/unwinding mechanism.

Interaction Curve for Shear and Torsion

A graph displaying the results from Column 8 with respect to shear and torsion interaction is shown in Figure 19. The procedure used for calculating the shear strength of Column 8 was the same as that used for the shear test specimens, i.e. the procedure developed by Tanaka and Park (2). The torsional strength for Column 8 was calculated using the procedures in ACI 318-89 (3) for rectangular beams. With respect to the shear and torsional strengths, it can be seen in the graph that the majority of the load applied to Column 8 was torsional in nature. The overstrength displayed for Column 8 is approximately 48%. The procedures for calculating the torsional strength of the oval column with interlocking spirals, while apparently conservative, are likely to be inexact. Further research into the behavior of interlocking spiral columns subjected to torsional load needs to be conducted, particularly in regard to rotation-direction bias resulting in unwinding of the spirals.

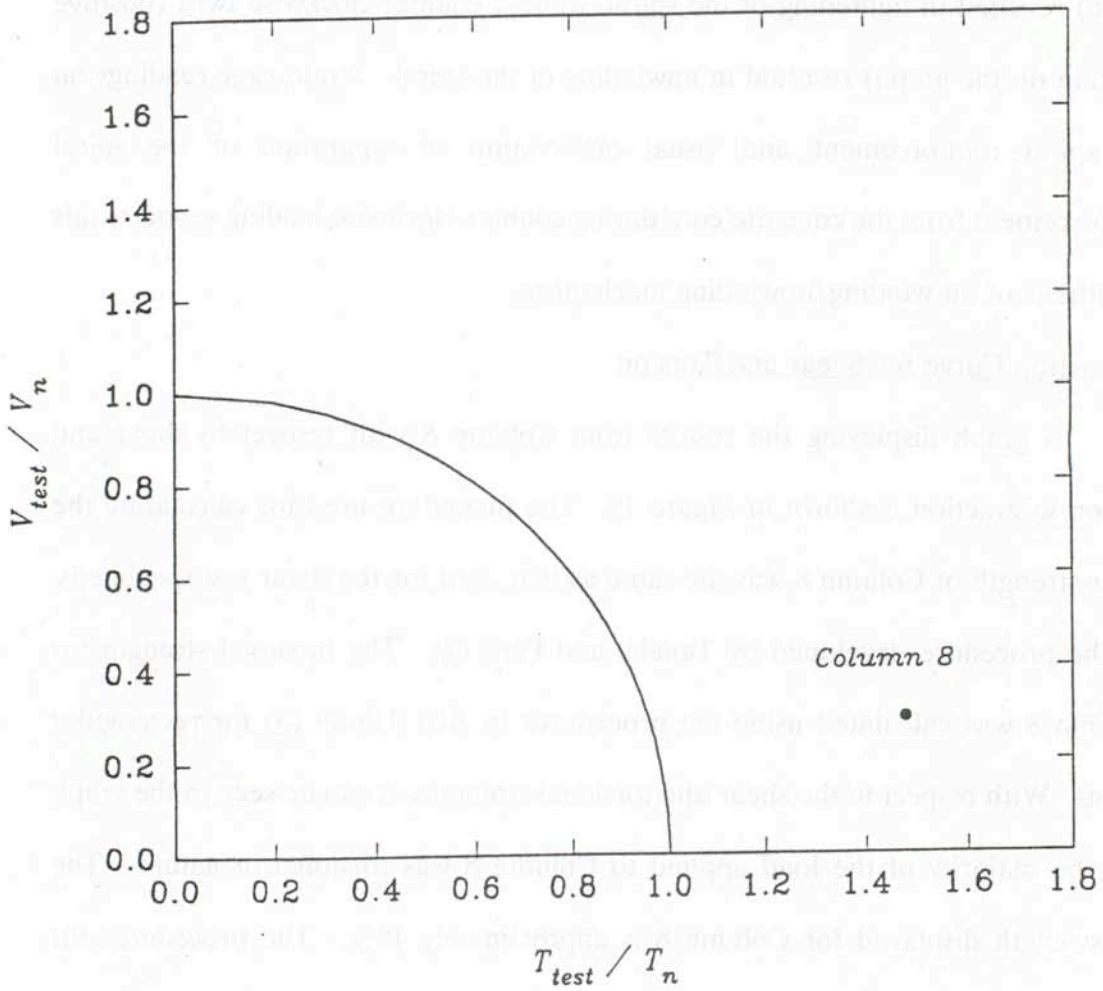

Figure 19 Shear-torsion interaction curve for Column 8.

REFERENCES

1. "Standard Specifications for Highway Bridges Relating to Seismic Design," adopted by the American Association of State Highway and Transportation Officials, Thirteenth Edition, 1983, with Revisions by the Office of Structures Design, California Department of Transportation, Sacramento, Calif., November, 1989.

2. Tanaka, H. and Park, R., "Use of Interlocking Spirals for Transverse Reinforcement in Bridge Columns," draft report, Department of Civil Engineering, University of Canterbury, New Zealand, 1990.

3. ACI Committee 318, "Building Code Requirements for Reinforced Concrete," ACI 318-89, American Concrete Institute, Detroit, Mich., 1989.

4. "Standard Specifications for Highway Bridges Relating to Seismic Design," adopted by the American Association of State Highway and Transportation Officials, Twelfth Edition, 1977, with Revisions by the Office of Structures Design, California Department of Transportation, Sacramento, Calif., November, 1979.

5. "Code of Practice for the Design of Concrete Structures, NZS 3101 Part 1:1982,"; "Commentary on the Design of Concrete Structures, NZS 3101 Part 2:1982,"; and "Amendment No. 1 to NZS 301:Parts 1 and 2, 1989," Standards Association of New Zealand, Wellington, New Zealand.

6. Buckingham, Grant C., "Seismic Performance of Bridge Columns With Interlocking Spiral Reinforcement," M.S. Thesis, Washington State University, Pullman, Wash., 1992.